Cu2Te-PVA as Saturable Absorber for Generating Q-switched Erbium-doped Fiber Laser

Harith b Ahmad (harith@um.edu.my)
Photonics Research Centre, University of Malaya https://orcid.org/0000-0002-9599-2086
Nur Fatini Azmy
Universiti Malaya
Siti Aisyah Reduan
Universiti Malaya
Norazriena Yusoff
Universiti Malaya
Zamzuri Abdul Kadir
International Islamic University Malaysia

Original Research

Keywords: Q-switched fiber laser, Copper telluride (Cu2Te), Saturable absorber, Wavelength tunable laser

Posted Date: February 4th, 2021

DOI: https://doi.org/10.21203/rs.3.rs-172432/v1

Version of Record: A version of this preprint was published at Optical and Quantum Electronics on March 30th, 2021. See the published version at https://doi.org/10.1007/s11082-021-02815-0.

Optical and Quantum Electronics (XXXX)XX:XXX
https://doi.org/XXXX/XXXX

Cu_2Te-PVA as Saturable Absorber for Generating Q-switched Erbium-doped Fiber Laser

Harith Ahmad[1,2,*] · Nur Fatini Azmy[1] · Siti Aisyah Reduan[1] · Norazriena Yusoff[1] · Zamzuri Abdul Kadir[3]

Received xxxxxx / Accepted: xxxxxx
Published xxxxxx

Abstract
A passively Q-switched erbium-doped fiber laser (EDFL) using copper telluride-polyvinyl alcohol (Cu_2Te-PVA) thin film as saturable absorber (SA) was proposed and demonstrated. The generated Q-switched pulses could be tuned over a tuning range of 44 nm from 1530 nm to 1574 nm, with the addition of a tunable bandpass filter (TBPF) into the C-band laser cavity. The pump power of 130.1 mW to 221.0 mW was used to observe the output pulses, which had repetition rates from 51.3 kHz to 61.7 kHz, with a minimum pulse width of around 1.84 µs and highest pulse energy of 7 nJ. The generated pulses were stable with a constant signal to noise ratio (SNR) value of around 51 dB when tested under continuous operation over a period of 60 minutes. To the best of our knowledge, this is the first demonstration of Q-switched pulses induced by a Cu_2Te-PVA based SA in an EDFL.

Keywords Q-switched fiber laser · Copper telluride (Cu_2Te) · Saturable absorber · Wavelength tunable laser

1 Introduction

Q-switched fiber lasers are highly attractive pulses sources for a variety of applications such as medicine, material processing, sensing, medicine and laser processing (Huang et al. 2014; Laroche et al. 2002) due to the many advantages that include low fabrication and operational costs, compact and robust form factor as well as being substantially easier to operate than their bulk optics counterparts. Q-switched lasing can be achieved by either active or passive techniques. Active Q-switching exhibits a benefit of being a system that are able to control the characteristics of the output pulses (Chen et al. 2014). However, this technique has the drawback of requiring sophisticated control electronics as well as the inclusion of additional components such as acousto-optic or electro-optic modulators into the system to generate Q-switched pulses, which can be rather expensive (Chen et al. 2014; Kim et al. 2017; Zhang et al. 2017). On the other hand, passive techniques allow for lower-cost, simpler and more compact systems to be realized. For this reason, passive technique is preferable by the researchers in generating a Q-switched pulses.

Saturable absorbers (SAs) were used as passive devices to generate Q-switched pulses in a fiber laser system as reported in previous works (Cheng et al. 2020; Nizamani et al. 2020; Xu et al. 2019; Siddiq et al. 2019; Haris et al. 2017). One of the earliest approaches is using semiconductor saturable absorber mirrors (SESAMs) (Li et al. 2012; Okhotnikov et al. 2003), which allowed the properties of the output pulses to be controlled. While being one of the most reliable techniques for the generation of Q-switched pulses, it also suffers from some shortcomings. For instances, it had a limited operating bandwidth, allowing to operate at only a particular wavelength, and also requiring substantially high fabrication and packaging costs. Additionally, this laser design also had a complex configuration, requiring careful optical alignment and also incurring a higher insertion loss. Thus, these limitations have encouraged and set off the researchers to

develop a simpler and cost-effective laser system (Okhotnikov et al. 2004; Cao et al. 2011; Li et al. 2014). Following this, breakthroughs in 2-dimensional (2D) and 3-dimensional (3D) materials such as carbon nanotubes and graphene have now opened up these materials for extensive use as SAs to generate short pulses in fiber laser system (Zhang et al. 2019; Solodyankin et al. 2008; Krylov et al. 2016; Wang et al. 2012). There are also other type of materials discovered as SAs, such as transition metal dichalcogenides (TMDs) (Chen et al. 2015), topological insulators (TIs) (Koo et al. 2017; Haris et al. 2017) and black phosphorus (Rashid et al. 2016; Zhang et al. 2020). These materials have been extensively explored as SAs to generate high performance and consistent Q-switched pulses in fiber lasers that are capable of operating over different optical wavelength regions such as C-band, S-band, O-band, 1 micron and 2 micron regions (Zhou et al. 2010; Ahmad,Reduan 2018; Ahmad et al. 2017; Hattori et al. 2016; Wang et al. 2019). Other than that, it should be also noted that many interesting self-pulsing laser dynamic were observed attributable to the signal repetition, excited-state absorption process (Upadhyaya et al. 2010; Tang,Xu 2010; El-Sherif,King 2002) or interactions among longitudinal mode oscillating in the laser cavity and stimulated Brillouin scattering (Peterka et al. 2018; Navratil et al. 2018; Kir'yanov et al. 2013).

In this study, material from group of transition metal chalcogenides (TMCs) have been used as an SA because of its unique optical characteristics that is suitable to be used in various applications such as photo-thermal conversion, photodetector, optical data storage and solar cells (Rao,Cheetham 2001; Green,O'Brien 1999; Wang et al. 2013). Copper telluride (Cu_2Te) from TMCs group have also found applications in the area of thermoelectric and ionic conductivity due to its high thermo-power values (Sridhar,Chattopadhyay 1998). A passively Q-switched erbium-doped fiber laser using Cu_2Te as SA is proposed and demonstrated in this work. The output pulses had a minimum pulse width of around 1.84 µs and could be tuned from 1530 nm to 1574 nm, with tuning range of 44 nm. The results of this proposed work shows that the capability of Cu_2Te as a broadband SA to generate a Q-switched pulses in erbium-doped fiber laser (EDFL) system.

2 Preparation and characterization of Cu_2Te-PVA saturable absorber (SA)

The SA in this work was fabricated using a simple solution casting technique. The precursor chemicals were commercially obtained and used without further purification. Following the typical recipe, the active element,

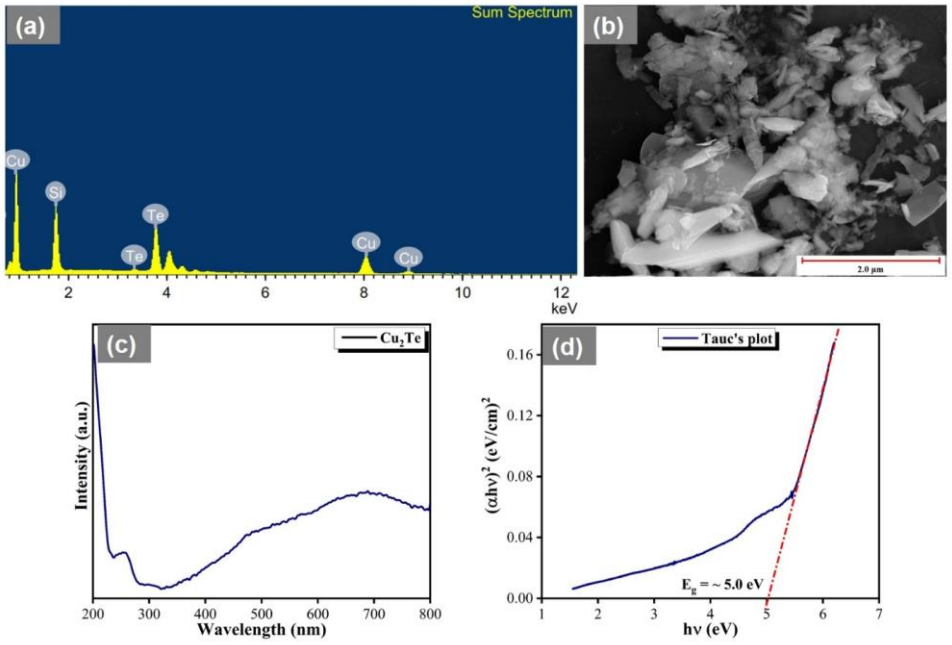

Fig. 1 Characterization of Cu_2Te: (a) EDX spectrum, (b) FESEM image, (c) UV-vis spectrum and (d) its corresponding Tauc's plot

which was the Cu_2Te powder was mixed in deionized water (DIW) and then sonicated to form a mixture with a homogeneous dispersion. The mixture was then further processed to remove any undissolved Cu_2Te particles, while the dissolved solution was extracted and then mixed with the polyvinyl alcohol (PVA) host. The PVA host with suspended Cu_2Te nanoparticles was dried to finally form the SA thin film. The detailed process for fabricating the Cu_2Te solution and PVA host has been explained in detail in other works.

A JEOL JSM 7600-F field emission scanning electron microscope (FESEM) linked to an energy dispersive X-ray (EDX) detector was utilized to characterize the surface morphology and elemental analysis of the Cu_2Te sample. The EDX spectrum of the Cu_2Te sample, which was dropped casted onto a silicon (Si) substrate, is shown in Figure 1(a). From the figure, several peaks can be seen which correspond to the copper (Cu), tellurium (Te) and Si elements. The Cu and Te peaks arise from the fabricated Cu_2Te sample while the presence of the Si peak is from the substrate. The strong peak intensity of Cu at ~ 1.0 keV and Te at ~ 3.8 keV is indicative of the purity of Cu_2Te sample. The surface morphology of the Cu_2Te sample is given in Figure 1(b). It can be seen from the FESEM image that the Cu_2Te comprises of a few Cu_2Te layers with a sheet-like structure stacked together, forming a thick sheet. The sheets have irregular sizes with lateral dimensions ranging from a few nm to 1.0 μm with random orientations as well.

The UV–visible (UV-vis) absorption spectrum of the Cu_2Te sample was obtained using a Varian Cary 50 UV–vis Spectrophotometer in order to study the optical properties and determine the band energy gap (E_g) of the Cu_2Te sample. Figure 1(c) shows the Cu_2Te optical absorption spectrum from 200 to 800 nm. The Tauc's plot of $(\alpha h\nu)^2$ versus $h\nu$ graph translated from the UV-vis spectrum of Cu_2Te is displayed in Figure 1(d). The absorption peak of Cu_2Te occured at wavelength of 257 nm and a broad peak at 681 nm. The peak at 257 nm is due to the transition from the p-bonding valence band (VB_2) to the p-anti bonding conduction band (CB_1) of Te (Sreeprasad et al. 2009). The value of E_g was determined according to the Tauc's equation as presented below:

$$\alpha h\nu = A(h\nu - E_g)^n \quad (1)$$

where α refer to the absorption coefficient, $h\nu$ is the photon energy, A is a proportion constant, n is 1/2 for a direct band gap and E_g is the optical band gap energy. The value for E_g is obtained by extrapolating the straight line portion of the curve to $(\alpha h\nu)^2 = 0$. The direct band gap of Cu_2Te sample is about 5.0 eV.

3 Experimental Setup

The setup of the proposed experiment is given in the Figure 2. The proposed experiment was configured based on a ring cavity fiber laser with the EDF act as a gain medium and Cu_2Te-PVA as a passive Q-switcher.

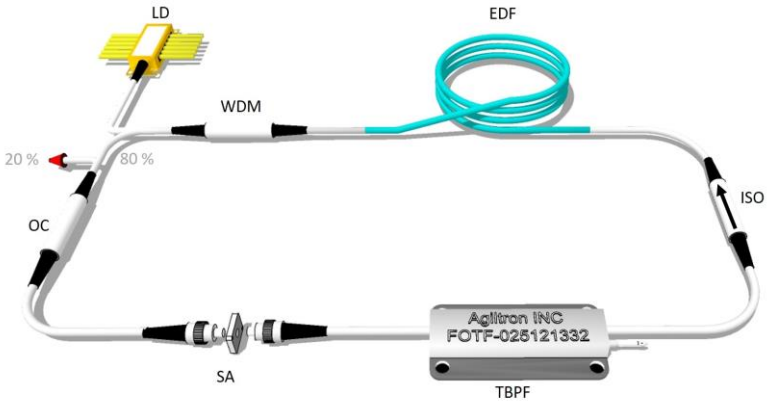

Fig. 2 Experimental setup for Q-switching in the EDF laser using the Cu_2Te-PVA based SA

A 980-nm LD was used to drive the EDFL and its signal was linked into the laser system through the common port of a 980/1550 nm fused wavelength division multiplexer (WDM). The output of the LD was connected to the 980 nm port of the WDM. Then output from the common port of WDM was channeled to the 0.9 m EDF, which had an absorption rate of 16 dB/m at 1530 nm and 11 dB/m at 980 nm, as well as a numerical aperture of 0.13 and mode-field diameter of 9.5 µm at 1550 nm. The output signal from EDF was then connected through an isolator to ensure the unidirectional propagation of the light in the laser system. Then, the signal passes through a tunable bandpass filter (TBPF), which allowed the central wavelength of EDFL to be tuned. The tuned output signal was linked to the SA assembly that was connected to an 80/20 optical coupler (OC), which extracted 20 % of the signal from the laser to be analyzed. The 80 % port was connected to the 1550 nm port of WDM, therefore completing the EDFL optical circuit. The total cavity length of the experimental setup was measured to be approximately 8.6 m.

The output signal was measured for its optical and pulse characteristics by using Anritsu MS9740A optical spectrum analyzer (OSA) and Yokogawa DLM2054 2.5 GS/s-500 MHz bandwidth oscilloscope (OSC). An Anritsu MS2683 Radio-Frequency Spectrum Analyzer (RFSA) was used to obtain the measurement in the frequency domain, while the output optical power was obtained by using a Thorlabs optical power meter (OPM).

4 Result and Discussion

Continuous wave lasing of the proposed system was observed without the Cu_2Te SA in the laser cavity. It can be seen that no pulses were generated based on this setting. When the Cu_2Te SA was placed in the laser cavity, the threshold power for a steady Q-switched was obtained at 130.1 mW up to a maximum pump power of 221.0 mW. Above a pump power of 221.0 mW, no Q-switched pulses were generated. This was most likely due to the SA becoming saturated, and as such only minimal signal absorption was possible at higher pump powers (Yap 2015). The dependence of the repetition rate, pulse width, pulse energy and average output power against the pump power is shown in Figure 3. Figure 3(a) shows the variation of the repetition rate and pulse width at different pumping powers. The repetition rate can be seen to increase from 51.3 kHz to 61.7 kHz while the pulse width decreases in an exponential manner from 4.5 µs to 1.8 µs as the pump power is raised from its threshold to maximum value. In addition, the pulse energy and average output power for different pump power are illustrated in Figure 3(b). Both quantities increase linearly with the pump power, with the pulse energy rising from 4.1 nJ to 7.0 nJ while the average output power increases from 0.21 mW up to 0.44 mW. The trend of both power-dependent characteristics are in a good agreement with previous reported works (Lü et al. 2019; Ahmad et al. 2016a). As observed when the pump power was decreased, the

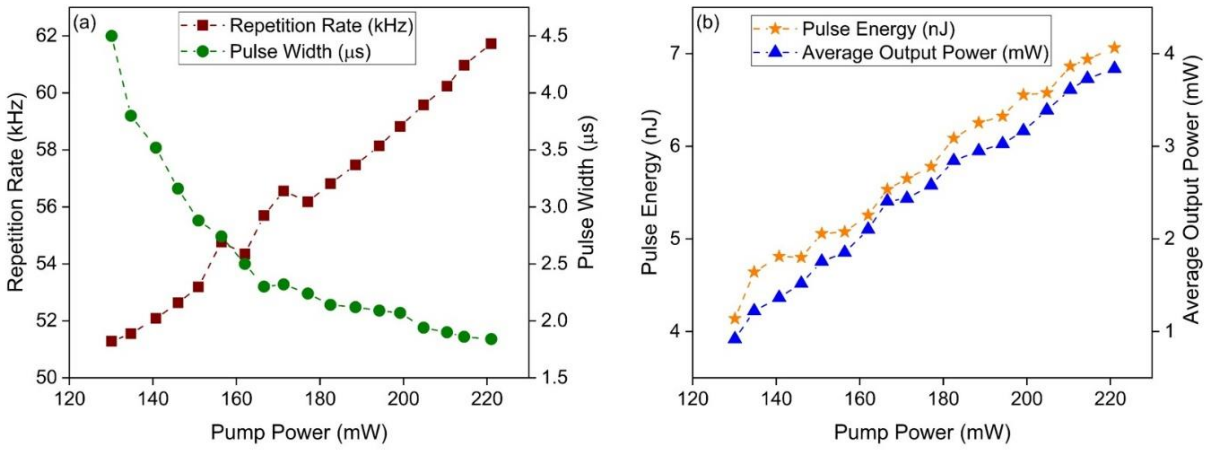

Fig. 3 (a) Repetition rate and pulse width and (b) pulse energy and average output power versus pump power

previously obtained trends reverse along the same path, indicating that the SA has not been damaged.

A detailed analysis of the Q-switched pulses is shown in Figure 4, taken at pump power of 166.6 mW, with Figure 4(a) showing the optical spectrum, with a central wavelength of 1562 nm. The pulse spectrum as shown in Figure 4(b) shows that the pulse train has a repetition rate of 55.7 kHz, corresponding to a period between pulses of 17.95 µs. The single pulse profile of the Q-switched output at this pump power is shown in Figure 4(c), and from the figure it can be seen that the pulses have a full width at half maximum (FWHM) of 2.3 µs. Radio frequency spectrum analysis was also undertaken to determine stability through its, as can been observed in Figure 4(d). The optical signal to noise ratio (SNR) was around 51 dB, indicating a highly stable output pulse.

The stability of the system was observed under continuous operation over a period of one-hour, with the output spectrum captured by the RFSA at 10-minutes interval. This is given in Figure 5(a) and shows that the output laser is stable without no drifting of the radio frequency value or intensity throughout the period of the stability test. The measured SNR value of around 51 dB and fundamental frequency also remained unchanged throughout the stability test as shown in in Figure 5(b). Therefore further indicates the stability of the laser cavity (Ahmad et al. 2018a).

By incorporating TBPF into the laser cavity, the Q-switched output from the laser could be tuned over a wavelength range of ~44 nm. As can be seen in Figure 6(a), at fixed pump power of 166.6 mW, the central lasing wavelength of the Q-switched pulses could be tuned from 1530 nm up to 1574 nm at increments of 2 nm. However, the gain spectrum of EDFL as well as intracavity losses limited the tunable range to only 44 nm, after which a pulsed output could no longer be observed. This limitation can be overcome by optimizing the cavity and using higher pump powers. The output power and repetition rate against different lasing wavelengths are shown in Figure 6(b). From the figure, it can be seen that the output power rises from 0.09 mW to 0.20 mW as the wavelength was increased from 1530 nm until 1560, after which it began to decrease from 0.19 mW to 0.16 mW as the wavelength continues to increase from 1564 nm to 1574 nm. It could therefore be inferred that the wavelength-dependence of the gain spectrum and intracavity loss plays a significant role in the characteristics of the output power and repetition rate of the system. In this regard, the strong intracavity lasing at high output powers will hasten the bleaching process of the Cu_2Te SA, resulting in a higher repetition rate (Wood,Schwarz 1967).

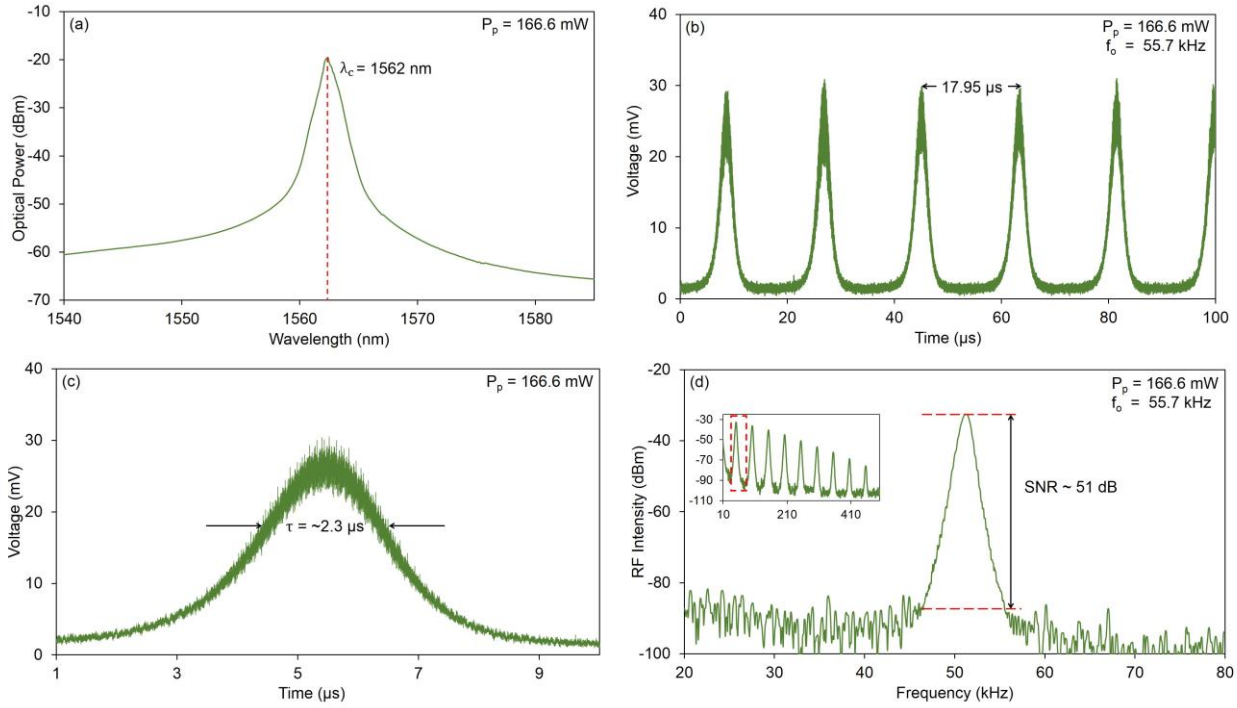

Fig. 4 Graph of Q-switched pulses characteristics in terms of (a) optical spectrum, (b) pulse train, (c) single pulse profile and (d) radio frequency (RF) spectrum

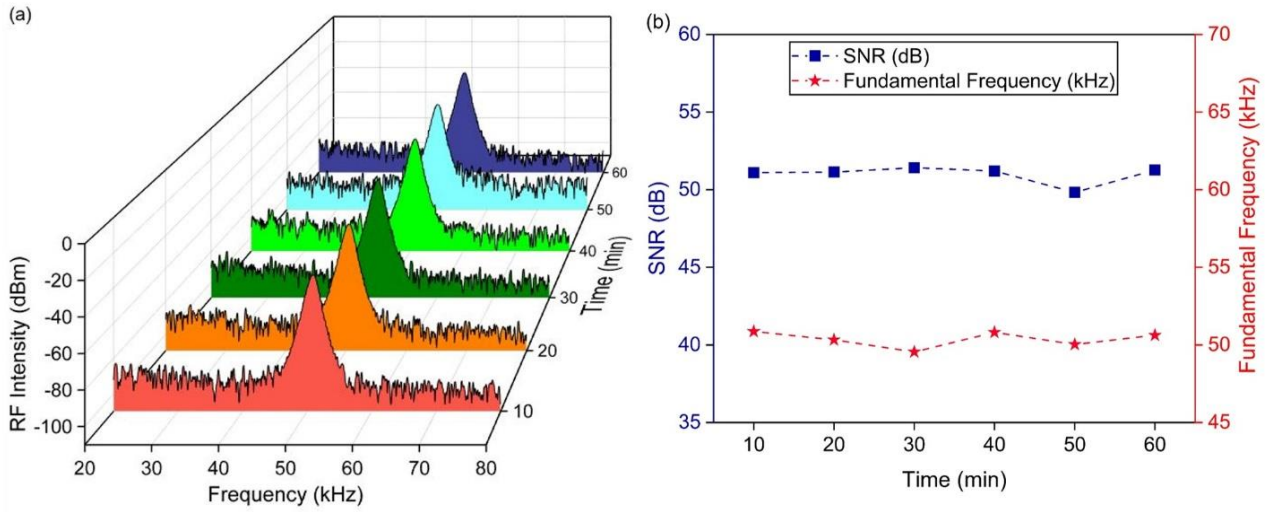

Fig. 5 (a) 3D plot of RF intensity and (b) SNR value and fundamental frequency from Q-switching operation over 1-hour of continuous operation

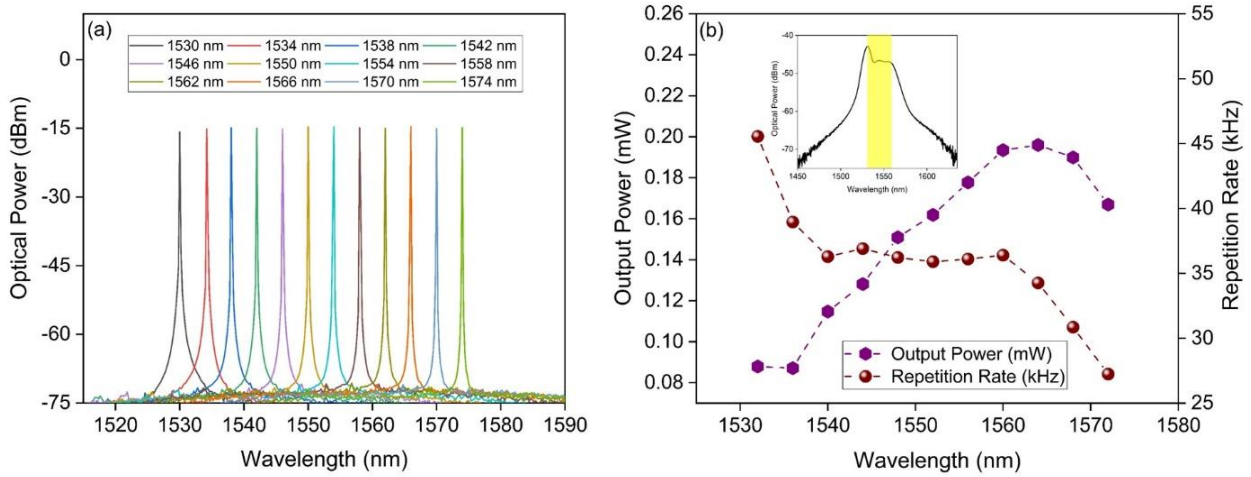

Fig. 6 Graph of (a) tunability output spectra of EDFL and (b) output power and repetition rate trend against tunable wavelength with ASE (inset)

Table 1 summarizes performances of reported works that deal with various SA. As tabulated in Table 1, the repetition rate of the proposed system was comparable to that of other similar works (Wang et al. 2012; Ahmad et al. 2018c; Ahmad et al. 2018b). While the work by Ahmad et al (Ahmad et al. 2016b) was able to generate outputs with a higher maximum repetition rate as well as higher maximum pulse energy, the system proposed in this work was able to generate output pulses with a smaller minimum pulse width that could be tuned along the C-band region. On the other hand, the SAs based on graphene (Wang et al. 2012) and In_2Se_3 (Ahmad et al. 2018c) were only able to generate output pulses with a lower maximum repetition rate and larger minimum pulse width as compared to our reported output pulses. Previous work using the WSSe based SA (Ahmad et al. 2018b), reported a comparable maximum repetition rate and tuning range with that of this work as well. Overall, the proposed system performs comparably to that of other similar optical laser cavities, with the output generated have the narrowest pulse width as well as the laser having the added advantage of wavelength tunability.

Table 1 Summary of different SAs performance in generating Q-switching

SA	Gain Medium	Central Wavelength (nm)	Max. Repetition Rate (kHz)	Max. Pulse Energy (nJ)	Min. Pulse Width (μs)	Tuning Range (nm)	Ref.
Graphene	EDF	1539.6	41.8	28.7	3.89	NA	(Wang et al. 2012)
WS_2	EDF	1560.7	84.8	9.8	3.84	NA	(Ahmad et al. 2016b)
In_2Se_3	Bi-EDF	1559.1	52	13.5	2.2	40	(Ahmad et al. 2018c)
WSSe	EDF	1568.4	61.8	7.31	2.6	40	(Ahmad et al. 2018b)
Cu_2Te	EDF	1562	61.7	7	1.84	44	This work

*NA= Not available, WS_2= Tungsten disulfide, In_2Se_3= Indium (III) selenide, WSSe= Tungsten sulphoselenide and Cu_2Te = Copper telluride

5 Conclusion

In this work, a Cu_2Te based SA was demonstrated to be able to induce Q-switching in the C-band region. Stable Q-switched pulses were observed at a threshold power of 130.1 mW up to a maximum pump power of 221.0 mW, with a maximum repetition rate of 61.7 kHz and minimum pulse width of 1.84 μs. The proposed laser had a tuning range of 44 nm across the C band region, from 1530 nm up to 1574 nm and showed high stability over a 60 minutes period of continuous operation. The SNR of the system was ~51 dB. The Cu_2Te based SA shows significant potential for use in the development of pulsed laser systems operating in the C-band region.

Declarations

Funding This work was supported by the University of Malaya [Grant Number RK 021-2019, TOP100PRC and RU002-2020] and the Ministry of Higher Education, Malaysia [Grant Number HiCoE Phase II Funding]

Conflicts of interest/Competing interests The authors declare that they have no known competing financial interests or personal relationships that could have appeared to influence the work reported in this paper

Availability of data and material Not applicable

Code availability Not applicable

References

Ahmad, H., Aidit, S., Thambiratnam, K., Tiu, Z.: Passively Q-switched O-band praseodymium doped fluoride fibre laser with PVA/graphene based SA. Electron. Lett. **53**(22), 1481-1483 (2017)

Ahmad, H., Aidit, S.N., Yusoff, N.: Bismuth oxide nanoflakes for passive Q-switching in a C-band erbium doped fiber laser. Infrared Phys Technol **95**, 19-26 (2018a)

Ahmad, H., Ismail, M.A., Suthaskumar, M., Tiu, Z.C., Harun, S.W., Zulkifli, M.Z., Samikannu, S., Sivaraj, S.: S-band Q-switched fiber laser using molybdenum disulfide (MoS_2) saturable absorber. Laser Phys Lett **13**(3), 035103 (2016a)

Ahmad, H., Reduan, S.A.: S+/S band passively Q-switched thulium-fluoride fiber laser based on using gallium selenide saturable absorber. Opt Laser Technol **107**, 116-121 (2018)

Ahmad, H., Ruslan, N., Ismail, M., Reduan, S., Lee, C., Sathiyan, S., Sivabalan, S., Harun, S.W.: Passively Q-switched erbium-doped fiber laser at C-band region based on WS_2 saturable absorber. Appl. Opt. **55**(5), 1001-1005 (2016b)

Ahmad, H., Tiu, Z.C., Ooi, S.I.: Passive Q-switching in an erbium-doped fiber laser using tungsten sulphoselenide as a saturable absorber. Chin Opt Lett **16**(2), 020009 (2018b)

Ahmad, H., Zulkifli, A.Z., Yasin, M., Ismail, M.F., Thambiratnam, K.: In_2Se_3 saturable absorber for generating tunable Q-switched outputs from a bismuth–erbium doped fiber laser. Laser Phys Lett **15**(11), 115105 (2018c)

Cao, W., Wang, H., Luo, A., Luo, Z., Xu, W.: Graphene-based, 50 nm wide-band tunable passively Q-switched fiber laser. Laser Phys Lett **9**(1), 54 (2011)

Chen, B., Zhang, X., Wu, K., Wang, H., Wang, J., Chen, J.: Q-switched fiber laser based on transition metal dichalcogenides MoS_2, $MoSe_2$, WS_2, and WSe_2. Opt. Express **23**(20), 26723-26737 (2015)

Chen, Y., Zhao, C., Chen, S., Du, J., Tang, P., Jiang, G., Zhang, H., Wen, S., Tang, D.: Large energy, wavelength widely tunable, topological insulator Q-switched erbium-doped fiber laser. IEEE J Sel Top Quantum Electrons **20**(5), 315-322 (2014)

Cheng, P.K., Tang, C.Y., Wang, X.Y., Zeng, L.-H., Tsang, Y.H.: Passively Q-switched and femtosecond mode-locked erbium-doped fiber laser based on a 2D palladium disulfide (PdS_2) saturable absorber. Photonics Res. **8**(4), 511-518 (2020)

El-Sherif, A.F., King, T.A.: Dynamics and self-pulsing effects in Tm^{3+}-doped silica fibre lasers. Opt. Commun. **208**(4-6), 381-389 (2002)

Green, M., O'Brien, P.: Recent advances in the preparation of semiconductors as isolated nanometric particles: new routes to quantum dots. ChemComm (22), 2235-2241 (1999). doi:10.1039/A904202D

Haris, H., Harun, S., Muhammad, A., Anyi, C., Tan, S., Ahmad, F., Nor, R., Zulkepely, N., Arof, H.: Passively Q-switched Erbium-doped and Ytterbium-doped fibre lasers with topological insulator bismuth selenide (Bi_2Se_3) as saturable absorber. Opt Laser Technol **88**, 121-127 (2017)

Hattori, H.T., Khaleque, A., Liu, L., Greck, M.R.: Ytterbium-doped Q-switched fiber laser based upon manganese dioxide (MnO_2) saturable absorber. Appl. Opt. **55**(32), 9226-9231 (2016)

Huang, Y., Luo, Z., Li, Y., Zhong, M., Xu, B., Che, K., Xu, H., Cai, Z., Peng, J., Weng, J.: Widely-tunable, passively Q-switched erbium-doped fiber laser with few-layer MoS_2 saturable absorber. Opt. Express **22**(21), 25258-25266 (2014). doi:10.1364/OE.22.025258

Kim, J., Koo, J., Lee, J.H.: All-fiber acousto-optic modulator based on a cladding-etched optical fiber for active mode-locking. Photonics Res. **5**(5), 391-395 (2017)

Kir'yanov, A.V., Barmenkov, Y.O., Andres, M.V.: An experimental analysis of self-Q-switching via stimulated Brillouin scattering in an ytterbium doped fiber laser. Laser Phys Lett **10**(5), 055112 (2013)

Koo, J., Lee, J., Lee, J.H.: Integrated fiber-optic device based on a combination of a piezoelectric transducer and a bulk-structured Bi_2Te_3 topological insulator for Q-Switched mode-locking of a fiber laser. J. Light. Technol. **35**(11), 2175-2182 (2017)

Krylov, A.A., Sazonkin, S.G., Arutyunyan, N.R., Grebenyukov, V.V., Pozharov, A.S., Dvoretskiy, D.A., Obraztsova, E.D., Dianov, E.M.: Performance peculiarities of carbon-nanotube-based thin-film saturable absorbers for erbium fiber laser mode-locking. J Opt Soc Am B **33**(2), 134-142 (2016)

Laroche, M., Chardon, A., Nilsson, J., Shepherd, D., Clarkson, W., Girard, S., Moncorgé, R.: Compact diode-pumped passively Q-switched tunable Er–Yb double-clad fiber laser. Opt. Lett. **27**(22), 1980-1982 (2002)

Li, H., Xia, H., Lan, C., Li, C., Zhang, X., Li, J., Liu, Y.: Passively Q-switched erbium-doped fiber laser based on few-layer MoS_2 saturable absorber. IEEE Photon. Technol. Lett. **27**(1), 69-72 (2014)

Li, J., Hudson, D.D., Liu, Y., Jackson, S.D.: Efficient 2.87 μm fiber laser passively switched using a semiconductor saturable absorber mirror. Opt. Lett. **37**(18), 3747-3749 (2012)

Lü, Y., Wei, C., Zhang, H., Kang, Z., Qin, G., Liu, Y.: Wideband tunable passively Q-switched fiber laser at 2.8 μm using a broadband carbon nanotube saturable absorber. Photonics Res. **7**(1), 14-18 (2019)

Navratil, P., Peterka, P., Vojtisek, P., Kasik, I., Aubrecht, J., Honzatko, P., Kubecek, V.J.: Self-swept erbium fiber laser around 1.56 μm. Opto-Electron Rev **26**(1), 29-34 (2018)

Nizamani, B., Jafry, A., Khudus, M.A., Memon, F., Shuhaimi, A., Kasim, N., Hanafi, E., Yasin, M., Harun, S.: Indium tin oxide coated D-shape fiber as saturable absorber for passively Q-switched erbium-doped fiber laser. Opt Laser Technol **124**, 105998 (2020)

Okhotnikov, O., Grudinin, A., Pessa, M.: Ultra-fast fibre laser systems based on SESAM technology: new horizons and applications. New. J. Phys. **6**(1), 177 (2004)

Okhotnikov, O., Jouhti, T., Konttinen, J., Karirinne, S., Pessa, M.: 1.5-μm monolithic GaInNAs semiconductor saturable-absorber mode locking of an erbium fiber laser. Opt. Lett. **28**(5), 364-366 (2003)

Peterka, P., Koška, P., Čtyroký, J.: Reflectivity of superimposed Bragg gratings induced by longitudinal mode instabilities in fiber lasers. IEEE J Sel Top Quantum Electron **24**(3), 1-8 (2018)

Rao, C.N.R., Cheetham, A.K.: Science and technology of nanomaterials: current status and future prospects. J. Mater. Chem. **11**(12), 2887-2894 (2001). doi:10.1039/B105058N

Rashid, F., Azzuhri, S.R., Salim, M.M., Shaharuddin, R., Ismail, M., Ismail, M., Razak, M., Ahmad, H.: Using a black phosphorus saturable absorber to generate dual wavelengths in a Q-switched ytterbium-doped fiber laser. Laser Phys Lett **13**(8), 085102 (2016)

Siddiq, N.A., Chong, W.Y., Pramono, Y.H., Muntini, M.S., Ahmad, H.: C-band tunable performance of passively Q-switched erbium-doped fiber laser using Tin (IV) oxide as a saturable absorber. Opt. Commun. **442**, 1-7 (2019)

Solodyankin, M.A., Obraztsova, E.D., Lobach, A.S., Chernov, A.I., Tausenev, A.V., Konov, V.I., Dianov, E.M.: Mode-locked 1.93 μm thulium fiber laser with a carbon nanotube absorber. Opt. Lett. **33**(12), 1336-1338 (2008)

Sreeprasad, T., Samal, A., Pradeep, T.: Tellurium nanowire-induced room temperature conversion of graphite oxide to leaf-like graphenic structures. J. Phys. Chem. C **113**(5), 1727-1737 (2009)

Sridhar, K., Chattopadhyay, K.: Synthesis by mechanical alloying and thermoelectric properties of Cu_2Te. J. Alloys Compd. **264**(1-2), 293-298 (1998)

Tang, Y., Xu, J.: Effects of excited-state absorption on self-pulsing in Tm^{3+}-doped fiber lasers. J Opt Soc Am B **27**(2), 179-186 (2010)

Upadhyaya, B.N., Kuruvilla, A., Chakravarty, U., Shenoy, M.R., Thyagarajan, K., Oak, S.M.: Effect of laser linewidth and fiber length on self-pulsing dynamics and output stabilization of single-mode Yb-doped double-clad fiber laser. Appl. Opt. **49**(12), 2316-2325 (2010)

Wang, H., Zuo, P., Wang, A., Zhang, S., Mao, C., Song, J., Niu, H., Jin, B., Tian, Y.: Facile synthesis and electrochemical property of Cu_2Te nanorods. J. Alloys Compd. **581**, 816-820 (2013)

Wang, J., Luo, Z., Zhou, M., Ye, C., Fu, H., Cai, Z., Cheng, H., Xu, H., Qi, W.: Evanescent-light deposition of graphene onto tapered fibers for passive Q-switch and mode-locker. IEEE Photon. J. **4**(5), 1295-1305 (2012)

Wang, M., Huang, S., Zeng, Y.-J., Yang, J., Pei, J., Ruan, S.: Passively Q-switched thulium-doped fiber laser based on oxygen vacancy MoO_{3-x} saturable absorber. Opt. Mater. Express **9**(11), 4429-4437 (2019)

Wood, O., Schwarz, S.: Passive Q-switching of a CO_2 laser. Appl. Phys. Lett. **11**(3), 88-89 (1967)

Xu, N., Ming, N., Han, X., Man, B., Zhang, H.: Large-energy passively Q-switched Er-doped fiber laser based on CVD-Bi_2Se_3 as saturable absorber. Opt. Mater. Express **9**(2), 373-383 (2019)

Yap, Y.K.: Chemical synthesis and characterization of graphene oxide for use as saturable absorber and broadband polarizer/Yap Yuen Kiat. University of Malaya (2015)

Zhang, C., Chen, Y., Fan, T., Ge, Y., Zhao, C., Zhang, H., Wen, S.: Sub-hundred nanosecond pulse generation from a black phosphorus Q-switched Er-doped fiber laser. Opt. Express **28**(4), 4708-4716 (2020)

Zhang, J., Kosugi, Y., Otomo, A., Nakano, Y., Tanemura, T.: Active metasurface modulator with electro-optic polymer using bimodal plasmonic resonance. Opt. Express **25**(24), 30304-30311 (2017)

Zhang, R., Wang, J., Liao, M., Li, X., Kuan, P.-W., Liu, Y., Zhou, Y., Gao, W.: Tunable Q-switched fiber laser based on a graphene saturable absorber without additional tuning element. IEEE Photon. J. **11**(1), 1-10 (2019)

Zhou, D.-P., Wei, L., Dong, B., Liu, W.-K.: Tunable passively Q-switched erbium-doped fiber laser with carbon nanotubes as a saturable absorber. IEEE Photon. Technol Lett. **22**(1), 9-11 (2010)

Affiliations

Harith Ahmad[1,2,*] · Nur Fatini Azmy[1] · Siti Aisyah Reduan[1] · Norazriena Yusoff[1] · Zamzuri Abdul Kadir[3]

Harith Ahmad
harith@um.edu.my

Nur Fatini Azmy
nfatinia24@gmail.com

Siti Aisyah Reduan
siti.aisyah@um.edu.my

Norazriena Yusoff
norazrienayusoff@um.edu.my

Zamzuri Abdul Kadir
zamzurikadir@iium.edu.my

[1] Photonics Research Centre, University of Malaya, 50603 Kuala Lumpur, Malaysia

[2] Physics Dept., Faculty of Science, University of Malaya, 50603 Kuala Lumpur, Malaysia

[3]Physics Dept. Kulliyyah of Science, International Islamic University Malaysia, 25200 Kuantan, Malaysia

Figures

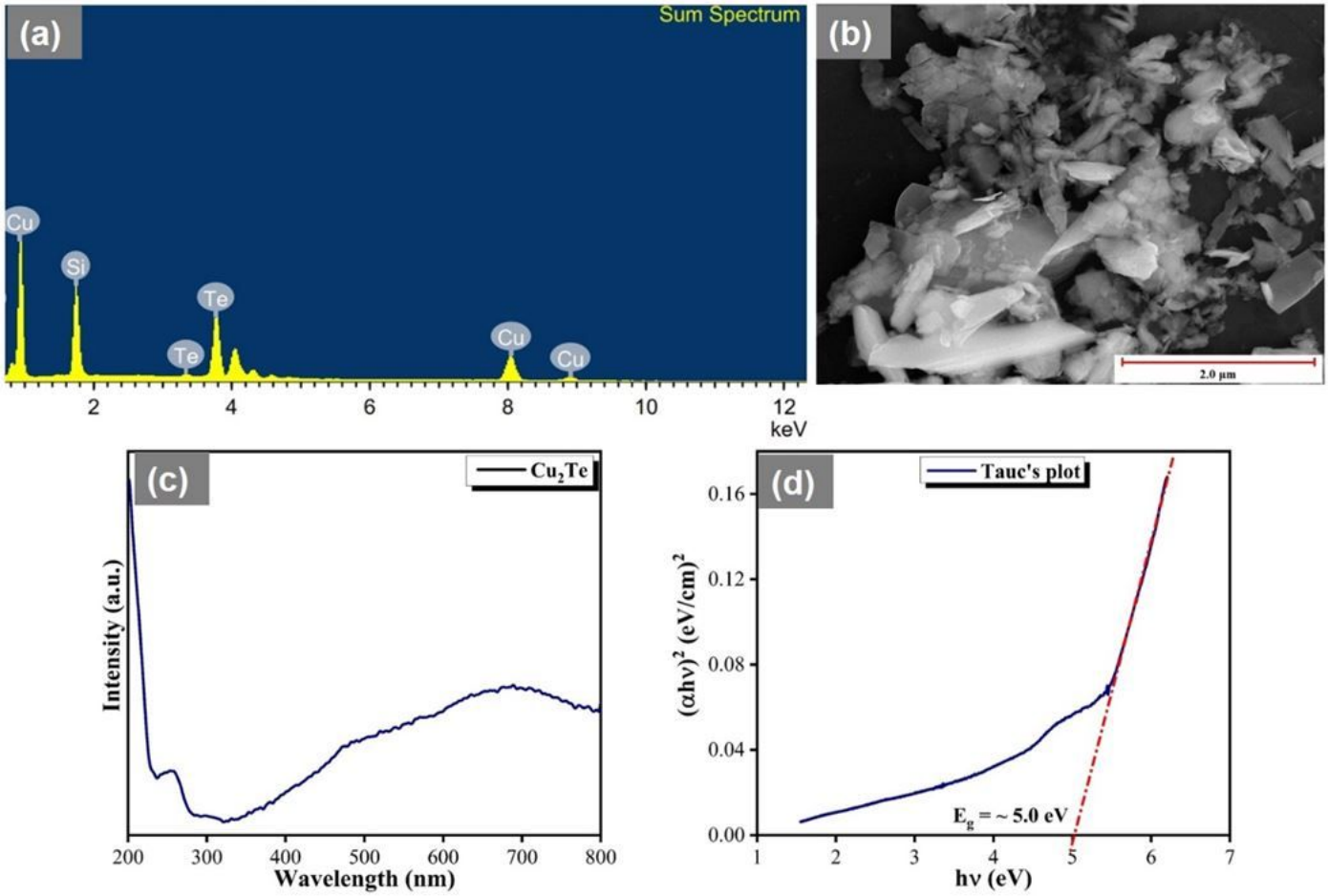

Figure 1

Characterization of Cu2Te: (a) EDX spectrum, (b) FESEM image, (c) UV-vis spectrum and (d) its corresponding Tauc's plot

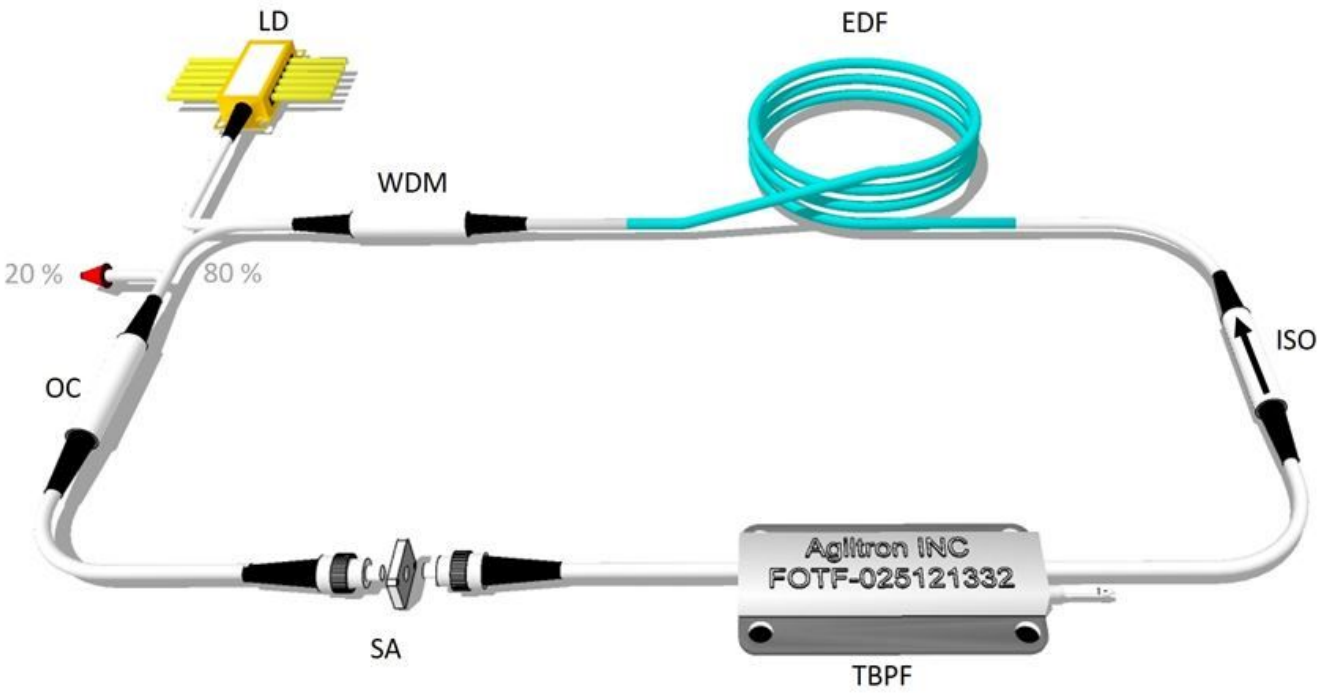

Figure 2

Experimental setup for Q-switching in the EDF laser using the Cu2Te-PVA based SA

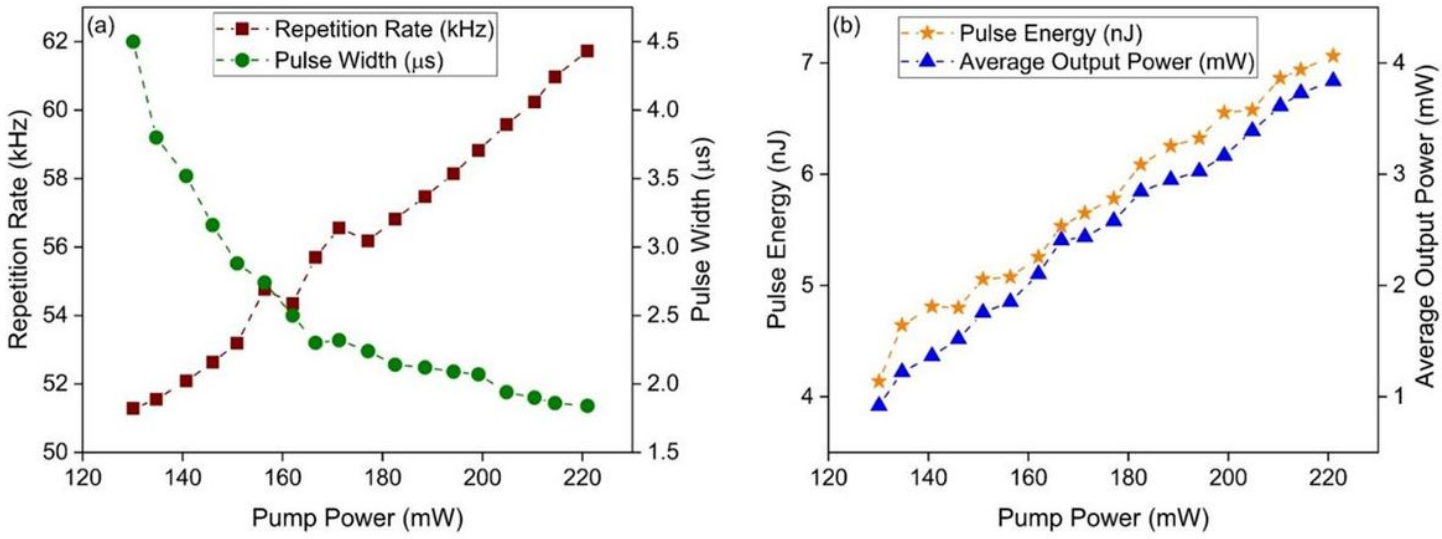

Figure 3

(a) Repetition rate and pulse width and (b) pulse energy and average output power versus pump power

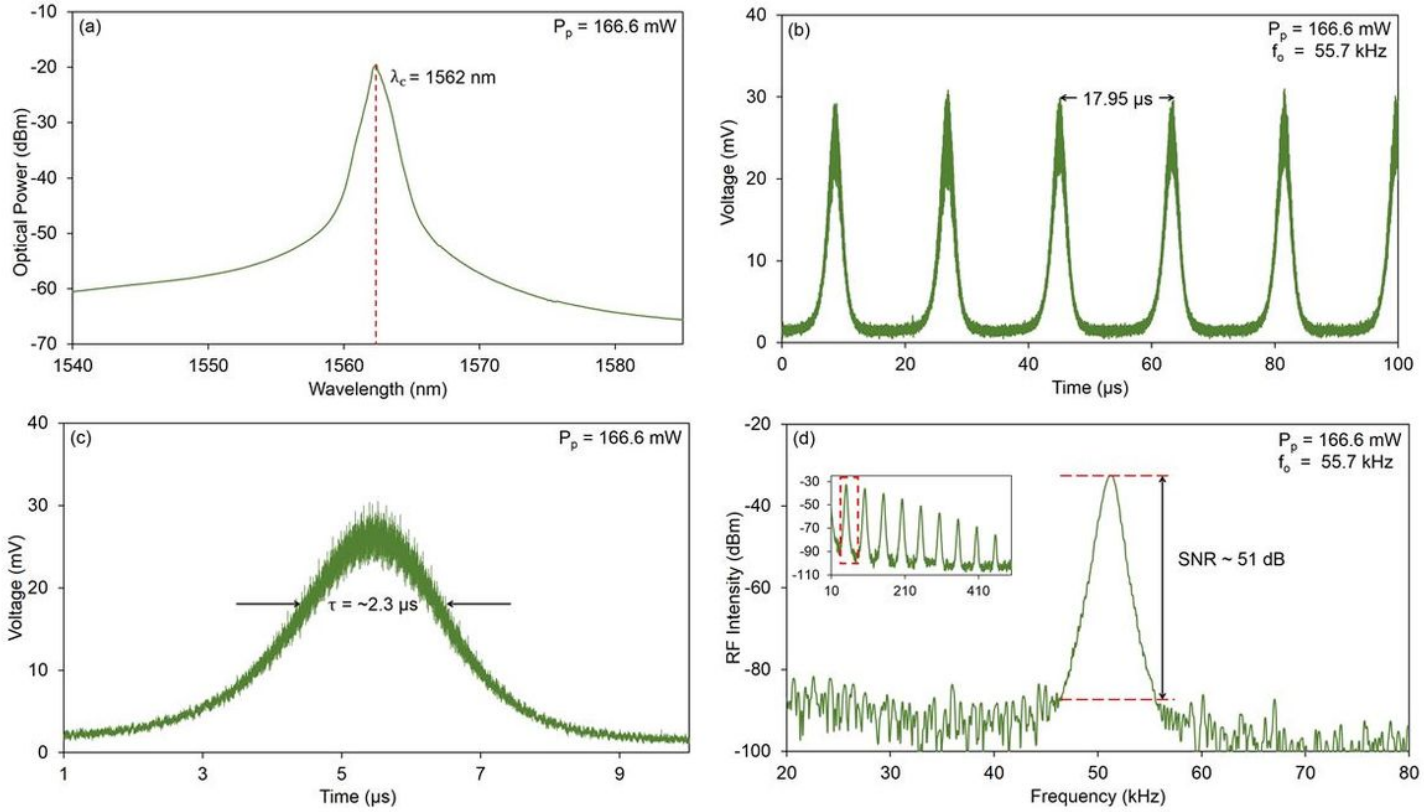

Figure 4

Graph of Q-switched pulses characteristics in terms of (a) optical spectrum, (b) pulse train, (c) single pulse profile and (d) radio frequency (RF) spectrum

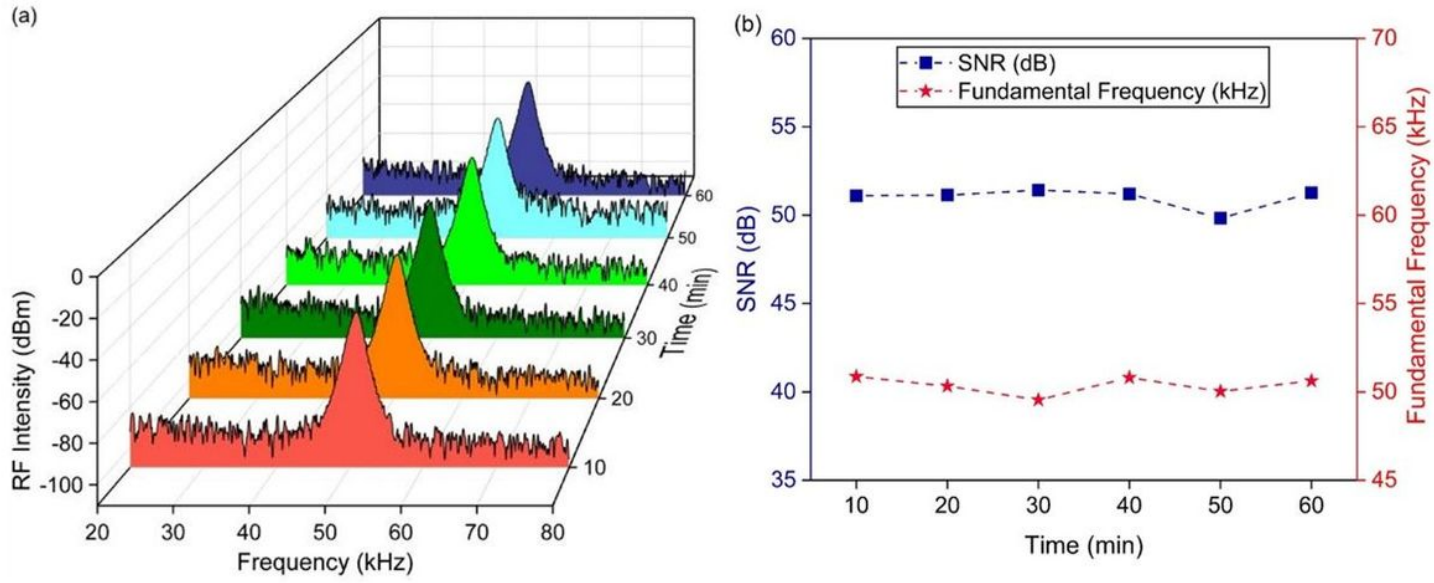

Figure 5

(a) 3D plot of RF intensity and (b) SNR value and fundamental frequency from Q-switching operation over 1-hour of continuous operation

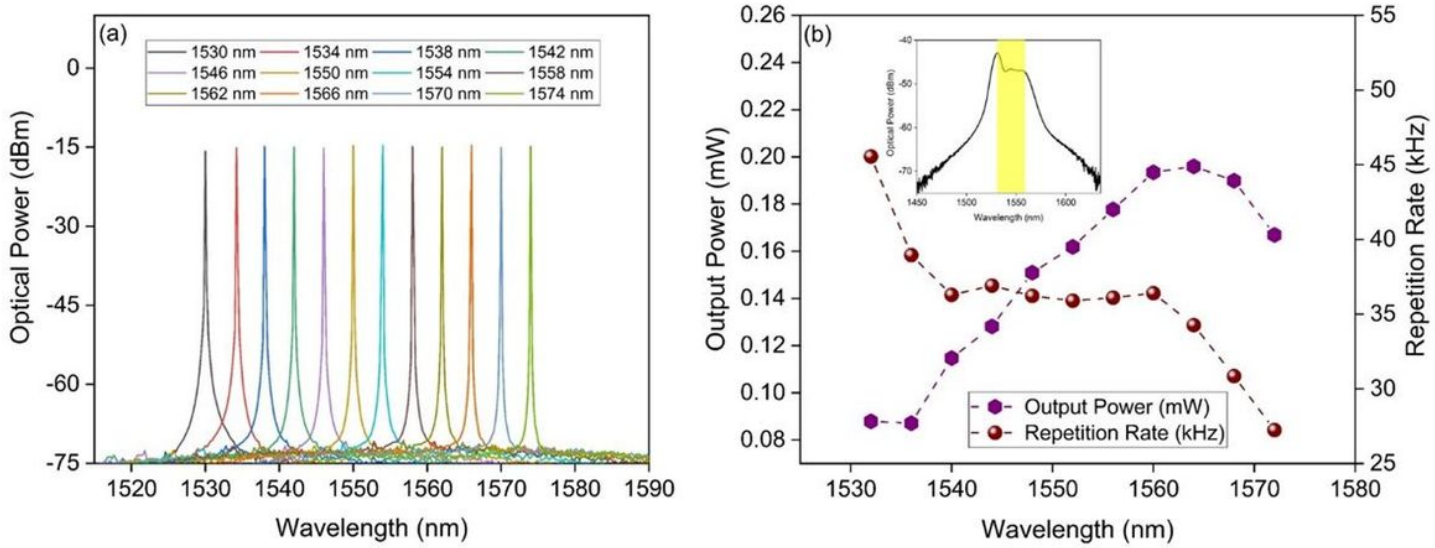

Figure 6

Graph of (a) tunability output spectra of EDFL and (b) output power and repetition rate trend against tunable wavelength with ASE (inset)